

Inter-model Comparison of Five Climate-Based Daylight Modelling Techniques: Redirecting Glazing/Shading Systems

Eleonora Brembilla^{1*}, Doris A Chi Pool², Christina J Hopfe¹, John Mardaljevic¹

¹School of Civil and Building Engineering, Loughborough University, UK

²Instituto Universitario de Arquitectura y Ciencias de la Construcción, Escuela Técnica Superior de Arquitectura, Universidad de Sevilla, Spain

*Corresponding author: E.Brembilla@lboro.ac.uk

Abstract

The evolution of building facades towards increasingly smarter and more complex fenestration systems required an evolution in simulation capabilities too. While simulation software can reliably reproduce the system's optical behaviour, the climate-based daylight evaluation of entire buildings needs to efficiently combine accuracy and computation speed. Five state-of-the-art Climate-Based Daylight Modelling (CBDM) techniques to evaluate a space with fixed venetian blinds are compared with each others. Multiple options to apply these techniques are also considered. The use of annual metrics based on global illumination led to a good agreement between all methods, while evaluating only direct sunlight exposed some profound differences between simulation techniques.

Introduction

Building facades are gradually evolving towards adaptive systems, responsive to variable climate conditions and to the occupants comfort necessities. Fenestration and shading devices are an essential part of any facade, providing beneficial natural daylight to the interior spaces and allowing views towards the outdoor, and as such, they are becoming more complex and varied too. For an energy saving or comfort improving strategy to be effectively determined at design stage, this complexity has to be reflected back into the performance analysis tools and to be adequately simulated and communicated. Climate-Based Daylight Modelling (CBDM) provides the framework for a complete, year-round, evaluation of the building luminous environment (Mardaljevic, 2000). Annual metrics have been defined for space characterisation and inserted into recent energy rating certificates, as well as mandatory design guidelines. Two examples are the latest LEED v4 (US Green Building Council (USGBC), 2013) and the Priority School Building Programme launched in the UK for the design of 260 new schools (Education Funding Agency, 2014). This prompted the development of a constantly evolving number of software that can perform CBDM (e.g.

DIVA-for-Rhino, OpenStudio, Groundhog), mainly based on the *Radiance* ray-tracer engine. This paper compares the results from five state-of-the-art *Radiance*-based techniques to perform CBDM, embedded in many of those pieces of software that offer a graphic user interface. On top of that, different options within the same techniques were also evaluated, namely three variations of the 3-phase method, two different approaches for the 5-phase method, and four different modes in DAYSIM. The evaluation scenario is a case study classroom from an ongoing research project (Drosou et al., 2016), on which fictitious shading systems have been applied for the present work.

Background: CFS and BSDF

The first techniques to perform CBDM by employing Daylight Coefficients (DCs) and the *Radiance* system (Ward Larson et al., 1998), such as the 4-component method and DAYSIM, were validated mainly for clear glazing, light shelves and diffuse elements (Mardaljevic, 2000; Reinhart, 2001). With the increasing diffusion of light redirecting systems, also called Complex Fenestration System (CFS), the available simulation tools faced a new challenge, that is to accurately describe the performance and the visual appearance of CFS. *Radiance* proved to be the most accurate tool to account for specular reflections (Tsangrassoulis and Bourdakos, 2003), as well as allowing for material descriptions that include angular dependent optical properties for re-diffusing systems (Reinhart and Andersen, 2006). However, the computation load that complex optics such as light-pipes or specular venetian blinds required for an accurate representation posed a limit to their insertion in annual simulations. A new methodology was proposed with the introduction of the 3-phase method (Saxena et al., 2010), purposely thought for fast annual evaluations that feature CFS and for parametric studies assessing multiple CFS options and configurations. By using Bidirectional Scattering Distribution Functions (BSDFs) to describe the CFS transmission and reflection behaviour, the simulation results can be obtained from the multiplication of three matrices: the View matrix (vmx), collecting values about the light redistribu-

tion in the interior space; the BSDF itself, generated on a Klems basis of 145 x 145 bins; and the Daylight matrix (dmx), collecting values about the exterior environment. This arrangement made possible the iterative substitution of any one of the three matrices without affecting the other two, accommodating the use of parametric analyses.

However, the increase in simulation speed came at the expenses of the accuracy in the description of the CFS. While for concept design stage and for comparative analyses, the 3-phase method could be considered fit-for-purpose, for more detailed results and for precisely modelled geometries the approximation was found to affect the overall accuracy (McNeil, 2013). The 5-phase method was therefore introduced to enable simulations of CFS at a higher accuracy. This was made possible by using: variable resolution BSDF, based on a Tensor Tree scheme, which can define light peaks transmission and reflections on finer solid angles; and assigning the direct sunlight contribution to 5185 point-like light sources, with a small solid angle (0.53 degrees) and evenly spread over the sky vault.

BSDFs based on the Klems scheme and encoded in an Extensible Markup Language (XML) file are becoming a widespread format, accepted by both daylight and thermal analysis simulation tools, such as *Radiance* and EnergyPlus (Lawrence Berkeley National Laboratory, 2013) respectively. They can be generated from existing databases, using for example Berkeley Lab WINDOW 6 (Mitchell et al., 2011) to assemble the required fenestration system, or via ray-tracing techniques, such as with the *Radiance* command *genBSDF*. This was experimentally validated within the 3-phase method validation (McNeil and Lee, 2013), as well as against another commercial ray-tracer, TracePro[®] (McNeil et al., 2013; Molina et al., 2015).

Simulation Methods

The following Section describes the five CBDM methods that were analysed and compared against each other in this work.

4-component method (4-cm)

The 4-component method employs the *Radiance* *rtrace* command in its original form to calculate the Daylight Coefficients (DCs), while the sky luminance distribution is obtained from blends of the CIE skies (Clear, Intermediate and Overcast) (Mardaljevic, 2000). This simulation method is based on a conceptual distinction between four daylight components, as each of them is derived using a slightly different process to maximise its accuracy. The four components are: Direct sunlight; Indirect sunlight; Direct skylight; Indirect skylight. The indirect components are obtained using *Radiance* stochastic sampling, with a Tregenza (i.e. 145 patches) sky division (Tregenza, 1987) formed by circular or rectangular

patches, for the indirect sunlight and indirect skylight respectively. The direct sunlight component is obtained from a deterministic calculation, as the ambient bounces (-ab) are set to zero and the sun is represented by one out of 2056 light point sources evenly distributed over the hemisphere. The direct skylight is obtained deterministically too (-ab 0), but using about 900 light point sources for each of the sky patches.

DAYSIM

DAYSIM is one of the most widespread back-end tools to perform CBDM. It implements a modified version of *rtrace* for the light redistribution simulation, called *gen_dc* in the legacy version 3.1e, and *rtrace_dc* in the latest version 4. The luminance distribution is derived from weather files data using the Perez All-Weather model.

The version currently embedded in most of commercial software is version 4, it uses the *rtrace_dc* command, and offers only the interpolation mode. Basically, the celestial hemisphere is divided as per Tregenza for the diffuse daylight coefficients and three ground segments according to Reinhart and Herkel (2000) for the ground daylight coefficients. Contributions from direct sunlight are modelled by up to 65 representative sun positions, depending on the location. Here, classical DAYSIM format picks, for any given date and time, the four representative sun positions which surround the actual sun position. Then, the contribution from the sun is distributed among these four 'sunlight coefficients' according to a weight, which considers the time and solar altitude of the actual and the four picked representative points.

When using version 3.1e, it is possible to select a finer representation of sky and sun, called Dynamic Daylight Simulation (DDS) (Bourgeois et al., 2008). This can be used in combination with the interpolation mode or with another option, the Shadow Test mode. The DDS format uses a new sky division scheme that distinguishes between contributions from various luminous sources as follows: 145 diffuse sky segments, one diffuse ground segment, 145 indirect solar positions and 2305 direct solar positions.

If a sensor is sunlit yet one or more of the four neighbouring positions is not in direct line of sight with the sensor, then the interpolation algorithm will systematically introduce errors as positions that do not see a sensor have direct/indirect solar contributions set of zero. To avoid this problem, the interpolated mode can be coupled with a shadow testing procedure: note is taken for each representative sun position, whether a sensor lies in its direct view (direct view=1) or not (direct view=0). For a given sky condition only those surrounding representative sun positions are considered whose direct view status equals the status of the actual sun position (Reinhart and Walkenhorst, 2001).

2-phase method (2-ph)

With the 2-phase method, instead of the classic *rtrace* command to simulate light behaviour, the new *rcontrib* (initially called *rtcontrib*) command was specifically introduced for annual simulations. The sun luminance is assigned to the three sky patches closest to the actual sun position and the sky subdivision can have variable resolution (according to Reinhart rather than Tregenza). The sun and sky contributions can therefore be accounted for in a single run and the computation load can noticeably diminish. Everything is stochastically sampled and the sun is defined with a *glow* material like the rest of the sky. However, in order for this method to work, the ambient interpolation has to be switched off (i.e. *-aa 0*, *-as 0*, *-ar 0*), giving rise to noisier images and requiring a higher number of ambient divisions (*-ad*).

3-phase method (3-ph)

In order to simulate the behaviour of CFSs, the 3-phase method was introduced on top of the 2-phase method, using the same *rcontrib* command, but splitting the raytracing process in two, one run for the exterior scene and one for the interior. The result matrices can be then multiplied to the matrix that describes the window BSDF material. This kind of function is generally built on a Klems basis hemisphere and is used to spatially relate the luminous flux coming from the exterior to the one transmitted by the window system itself towards the interior (McNeil and Lee, 2013).

5-phase method (5-ph)

The 5-phase method takes the results from the 3-phase method, subtracts the direct sunlight component as it was calculated with the 3-ph, and re-simulates it using 5185 point-like sources evenly distributed over the hemisphere and applying a variable resolution Tensor-Tree BSDF material instead of the Klems one; in this way, peaks of light can be traced more reliably from the sun position and then accurately accounted for at the window transmission step (McNeil, 2013).

Methodology

A classroom space was chosen as case study and modelled in SketchUp. As shown in Figure 1, the space is sidelit from a curtain-wall that occupies a complete side of the room. This aperture was oriented towards South, to simulate a space where there is an effective need for a shading strategy. Standard reflectance values were applied on the model surfaces. Horizontal venetian blinds were added to the model, placed on the interior side of the windows and within the sill depth. The slats were modelled as simple horizontal surfaces, with zero thickness, 50 mm wide and spaced every 40 mm; their reflectance value was 0.62 and for this study they were treated as perfected diffusers. The 3D model had to be modified to meet the require-

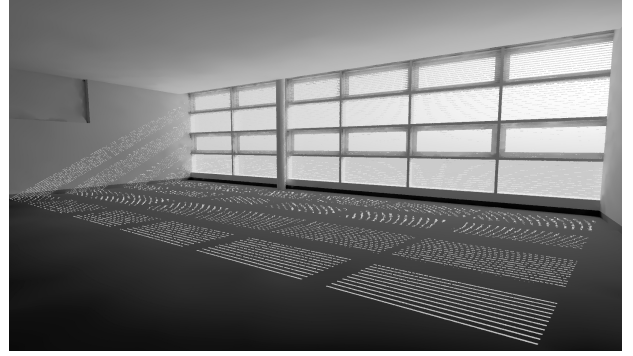


Figure 1: Rendering of the classroom with sunny sky conditions on the 1st March at 13:00, generated with Radiance. The curtain wall visible in the image is oriented towards South. Fixed venetian blinds were inserted on the interior side of the glazing, within the sill depth.

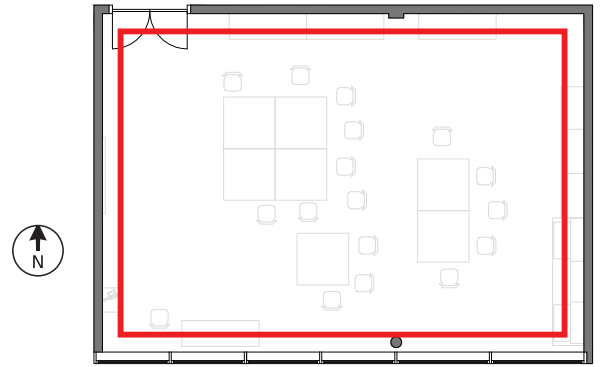


Figure 2: Plan view of the classroom (dimensions: 11.2 x 7.9 m). The space is side-lit from the South facade. The edge of the working plane used for the analyses further on is signed in red and runs at a 0.50 m distance from the room perimeter.

ments of some of the simulation methods. While for DAYSIM, the 4-component and the 2-phase methods all the elements of the room and of the shading system were explicitly modelled, the 3- and 5-phase methods required different approaches.

Three different ways of employing the 3-phase method were considered. In the first one (case D1), the curtain-wall was completely replaced by two surfaces enclosing the wall depth. The surface that faces the interior of the room acts as a receiver for the rays traced from the virtual sensors, while on the exterior side further rays originate from points randomly distributed over the exterior surface and are sent towards the sky vault. The behaviour of the fenestration system originally enclosed within those two surfaces was represented by a BSDF instead. The BSDF was generated by using the *Radiance* command *genBSDF* and it was created on a Klems basis. In the second and third cases, the frame geometry was explicitly modelled, while the glazing and venetian blinds

combined system was represented with a zero thickness BSDF; in one case the BSDF was created using *genBSDF* (case D2), while in the other case it was generated in Window 6.3 (case D3).

For the 5-phase method, two different procedures were adopted: with and without proxied geometry. For the option without proxied geometry (case E1), a surface was placed on the interior side of the curtain-wall (the same as the internal surface created for the 3-phase method in case D1) and the actual fenestration geometry was not modelled. A BSDF material was assigned to that surface, where the BSDF definition was created by using *genBSDF* but specifying the flag (-t4 5) for a Tensor Tree basis. For the option with proxied geometry (case E2), the same steps were followed, but keeping in the model the actual geometry for windows and venetian blinds; this required the specification of the system's thickness in the BSDF material definition, so that only direct rays were blocked by the proxied geometry, while indirect rays bypassed it.

The three BSDF that resulted from *genBSDF* runs were generated as follows, for cases D1, D2 and E respectively, with all simulation parameters left as per default:

```

1 genBSDF -n 4 -geom meter L3-v01.mat
  curtwall_vblinds.rad > curtwall_venblinds.xml
2 genBSDF -n 4 -geom meter -dim 1.0 1.2 0.27
  0.47 -0.2 0 L3-v01.mat glazing.rad
  venetianblinds.rad >! int_venblinds.xml
3 genBSDF -n 4 -t4 5 -geom meter L3-v01.mat
  curtwall_vblinds.rad >
  curtwall_venblinds_t45.xml

```

Except for the generation of the BSDFs, all the other ambient parameters were set following a convergence test for each of the methods under analysis. The test was based on the agreement of the Total Annual Illumination (TAI) values obtained from multiple simulation runs. This specific metric was selected as it was deemed to be more sensible to changes in parameters than other annual metrics such as Daylight Autonomy (DA) or Useful Daylight Illuminance (UDI); the convergence of annual metrics is obviously reached more easily than if it was tested for instantaneous conditions or for visualisation purposes, but for the scope of this work it was considered accurate enough. The ambient parameters eventually used are reported in Table 1.

After this preliminary calibration of the simulation settings, CBDM evaluations on the case study room were performed with each method and the annual metrics so obtained compared with each others, for a total of eight cases:

- A** 4-component method;
- B** DAYSIM v4;
- C** 2-phase method;
- D1** 3-phase method with thick BSDF, from genBSDF;

D2 3-phase method with zero thickness BSDF, from genBSDF;

D3 3-phase method with zero thickness BSDF, from Window6;

E1 5-phase method without proxied geometry;

E2 5-phase method with proxied geometry.

An additional evaluation was carried out among the different modes that DAYSIM offers, but the grid of virtual sensors had to be coarser (1.00 m spacing) and the ambient parameters lower (-ab 3), as a trade-off between accuracy and computation times.

B1 DAYSIM v4 with interpolation mode;

B2 DAYSIM v3.1e with interpolation mode;

B3 DAYSIM v3.1e with DDS option and interpolation mode;

B4 DAYSIM v3.1e with DDS option and shadow testing mode.

In all of them, the occupancy schedule was set to be 8:00-18:00 and the weather file used was the EPW for London Gatwick. A sensor grid spacing of 0.25 m was used for the first inter-model comparison, and of 1.00 m for the second one, with both sensor planes set at 0.80 m high.

The simulation results were expressed with CBDM annual metrics that are currently required by the aforementioned design guidelines, i.e. Priority Schools Building Programme (PSBP) and LEEDv4: Useful Daylight Illuminance (UDI) with thresholds at 100, 300 and 3000 lx; Annual Sunlight Exposure (ASE) with thresholds at 1000 lx and 250 hours; and DA with threshold at 300 lx (instead of Spatial Daylight Autonomy (sDA), which was always equal to 100%). TAI was included too, as it helped to highlight some differences between techniques that were not discernible from other metrics.

For the annual metrics that resulted to be significantly different, an additional analysis was carried out, looking at all the illuminance profiles obtained from the simulations. In particular, as the main differences were found to be in ASE results, the analysis

Table 1: Radiance ambient parameters set for each method.

4-cm	-ab 5 -ad 2048 -ar 128 -as 256 -aa 0.2 -lw 5e-3
DAYSIM v4	-ab 5 -ad 4096 -ar 512 -as 512 -aa 0.2 -lw 4e-3
DAYSIM v3.1e	-ab 3 -ad 4096 -ar 512 -as 512 -aa 0.1 -lw 4e-3
2-ph	-ab 5 -ad 89600 -lw 1e-5
3-ph (vmx)	-ab 5 -ad 22400 -lw 5e-5
3-ph (dmx)	-ab 2 -ad 22400 -lw 5e-5
5-ph	-ab 1 -ad 89600 -lw 1e-5 -dc 1 -dt 0 -dj 1 -st 1 -ss 0

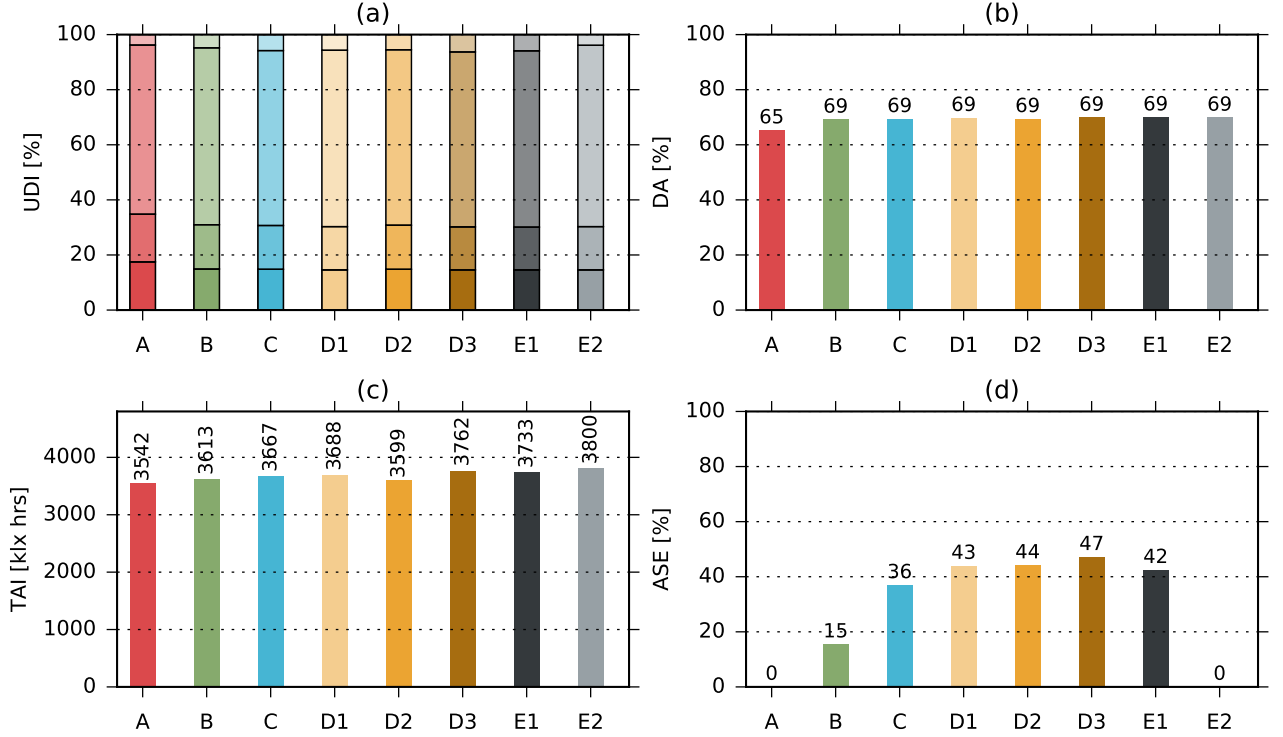


Figure 3: Annual CBDM metrics for each of the considered cases. The spacing between virtual sensor points for these simulations was 0.25 m. Graph (a) shows UDI results averaged over the working plane, where the stack bars represent the four UDI ranges, from bottom to top: UDI-n ($E < 100$ lx); UDI-s (100-300 lx); UDI-a (300-3000 lx); UDI-x ($E > 3000$ lx). Graph (b) shows DA results averaged over the working plane, with threshold equal to 300 lx. Graph (c) shows TAI, the cumulative result of illuminance values during occupancy period. Graph (d) shows ASE, calculated from direct sunlight with a threshold of 1000 lx for 250 hours.

focused on the illuminance profiles containing data from the direct sunlight contribution only.

Results

The first set of results is showed in Fig. 3. Graph (a) reports all UDI results, for the four different ranges: UDI-n ($E < 100$ lx); UDI-s (100-300 lx); UDI-a (300-3000 lx); and UDI-x ($E > 3000$ lx). All the considered methods agree well, within a maximum difference range of 5%. The most substantial differences can be found in the UDI-n range for the 4-component method, which is higher than all the others (UDI-n = 18% rather than 15%); and in the UDI-x range of the 4-component method and the 5-phase method that used proxied geometry, which are slightly smaller in compare with the rest (UDI-x = 4% rather than 6%). Graph (b) reports DA results, which are very consistent throughout all simulation techniques, with only the 4-component method reporting a slightly lower value (DA = 65%, rather than 69%). Graph (c) shows the cumulative results in TAI, with the 4-component method adding up to the smallest value (3542 klx hr) and the 5-phase method that used proxied geometry adding up to the highest value (3800 klx hr). Last, graph (d) shows the results for ASE, which is the metric that was found to be the most sensitive

to the variation in simulation techniques. Values go from being equal to zero (4-component method and 5-phase method with proxied geometry), up to 47% for the 3-phase method that used a BSDF with thick geometry. ASE is calculated from illuminance values deriving exclusively from the direct sun contribution; this is where the simulation techniques differ the most between each others, therefore the large differences in ASE results.

To understand better the reasons behind the discrepancies found in the ASE results, the histogram in Fig. 4 attempts to clarify the frequency distribution of all the instances and all the virtual sensors where direct light was recorded for each of the methods. All the data higher than zero were grouped in bins of 4000 lx size, to show how many sensors recorded a specific range of illuminances throughout the year. It is possible to recognise two main behavioural groups: the 2-phase method (C), all three versions of the 3-phase method (D1, D2, D3) and the 5-phase method without proxied geometry (E1) present a peak at lower values (0-4000 lx range), while quickly dropping around the 10.000 lx ranges; on the other hand, the 4-component method (A), DAYSIM (B) and the 5-phase method with proxied geometry (E2) are characterised by slowly decreasing value ranges that reach

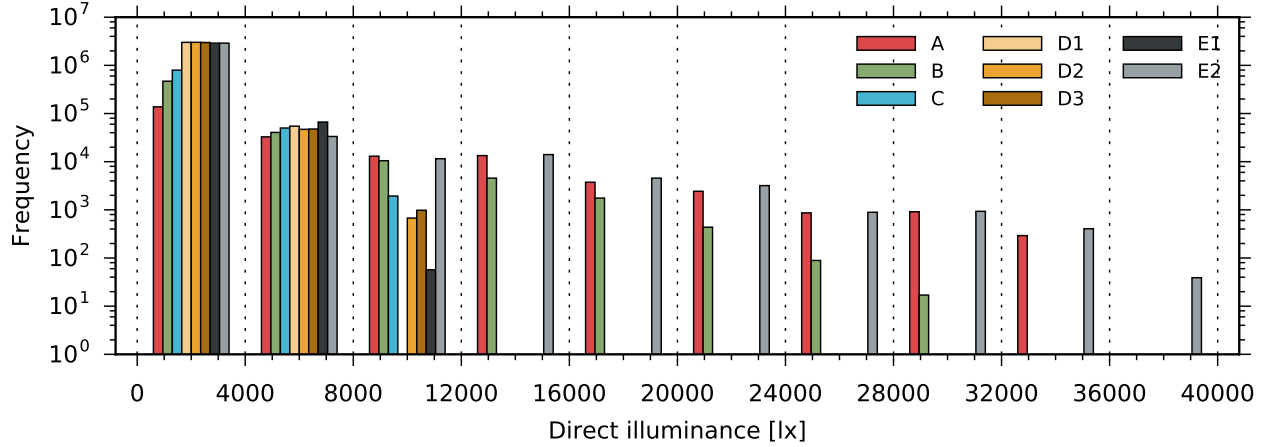


Figure 4: Histograms of the direct illuminance results obtained from the eight simulation procedures considered. The null values were excluded from the plotted data and the remaining values were binned in groups of 4000 lx.

up to 37.000 lx. The 5-phase method with proxied geometry (E2), in particular, is the one with the widest range of values, with many low intensity instances and the highest intensity ones at the same time.

To further illustrate the difference in the distribution of direct illuminance profiles, two specific instances when direct light struck into the space were plotted, as shown in Fig. 5 and 6. These two points in time were chosen by picking one instance where the 4-component method recorded illuminances lower than 4000 lx (therefore falling within the first bin of the histogram in Fig. 4) and one where it recorded illuminances higher than 32000 lx (therefore falling in the last part of the histogram).

From the plots, it is possible to notice the profound difference in how each simulation method treats the direct contribution. The 4-component method is characterised by very intense and defined light patches peaking in through the shading system; however, it should be noticed that, as the gaps between venetian blinds are closer together (0.04 m) than the space between virtual sensors (0.25 m), a good portion of direct sunlight that is entering the space is not recorded. DAYSIM shows defined patches, of slightly lower intensity and coming from different directions, as there are four sunlight sources represented on the sky vault. The 2-phase method results in ‘blurred’ patches of light larger than the projection that the glazing would cast on the horizontal plane, although the window frames can be recognised from the pattern. The 3-phase method that used a BSDF material with thickness (case D1) lost the definition of the fenestration system’s shape completely and resulted in a single large light patch; the 3-phase method versions that used a BSDF with no thickness (case D2 and case D3) held similar outcomes, independently of the source of the BSDF. The 5-phase method that did not use proxied geometry had a single patch of light, but with clearer edges than the 3-phase method; last, the

5-phase method with proxied geometry shows a combination of highly concentrate light peaks and a larger presence of re-diffused, low intensity, light around the room.

Under the plots, the sum of the illuminance values at each sensor cell in that particular instance is reported. This helps to understand how the total amount of energy transmitted inside the room is very similar, independently of the simulation technique. The difference lies in the redistribution of this energy; some techniques are able to reproduce the transmission of high peaks of concentrated light, while others are smearing out those peaks over larger areas, or multiple points. These ‘light spreads’ happen either at the sky/sun description level (DAYSIM, 2-ph), or at the fenestration system level (5-ph), or at both (3-ph).

Fig. 7 shows the results obtained from different DAYSIM modes, using a coarser grid with 1.00 m spacing between virtual sensors. All the techniques agree well with each others, with small differences for most of the annual metrics. However, the spacing is thought to have played a role in smoothing out the differences; if the two cases B and B1 (0.25 m and 1.00 m spacing respectively) are considered, it is possible to find a relevant difference in ASE results (15.4% against 1.4%), even if the simulation technique employed was exactly the same. ASE is likely to be highly dependent on the analysis grid resolution. The lower simulation ambient parameters are not influencing ASE results, as they are run with ambient bounces always at zero, to account for the direct light only. TAI is the metric that is mostly affected by insufficient ambient parameters settings, as it can be seen from the difference between cases B and B1, where the ambient bounces were set at 5 and 3 respectively; by contrast, DA and UDI are not influenced by this. The Shadow Test mode (case B4) returned lower results than the other DAYSIM modes, for example when looking at the UDI-x range or at TAI results.

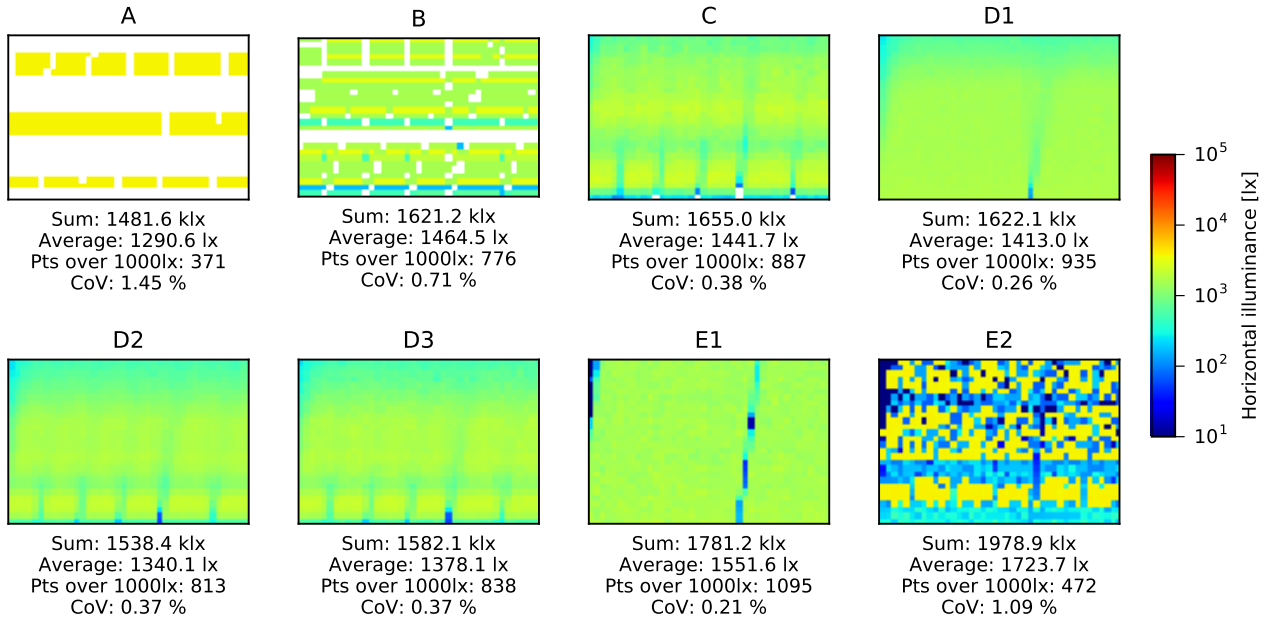


Figure 5: Falsecolor plots of the horizontal virtual plane placed in the room at 0.8 m height. The plots show the direct illuminance simulated on the analysis grid at a specific instant (9th January h 12:00), for each of the analysed CBDM methods. This point in time was chosen as it illustrates the difference between methods when the illuminance values are relatively low (< 4000 lx).

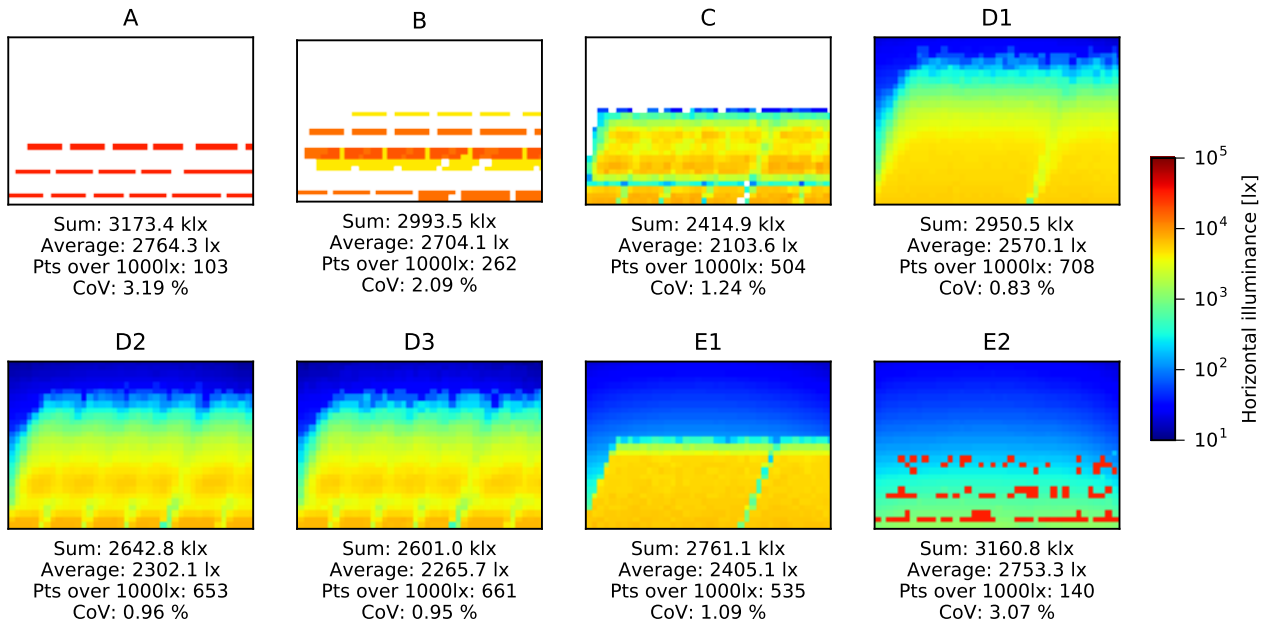


Figure 6: These plots show the direct illuminance for the 1st March at 13:00, for each of the analysed CBDM methods. This instant represents an instance in which the illuminance values obtained from the 4-component method are high (> 32.000 lx).

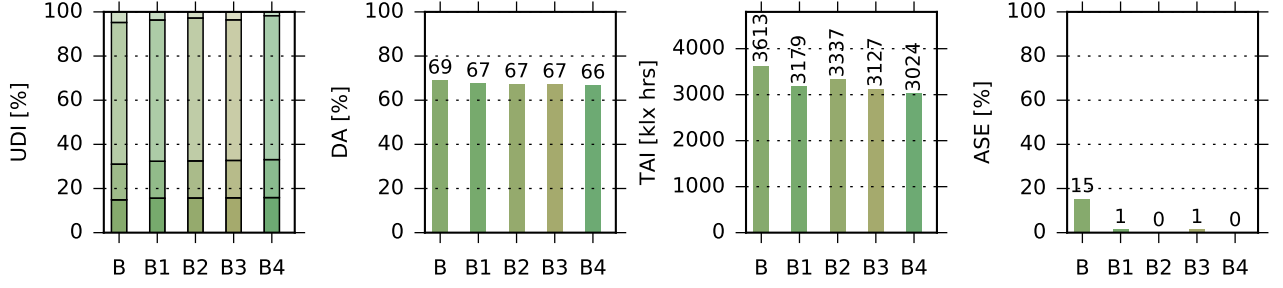


Figure 7: Annual CBDM metrics obtained with four different modes available in DAYSIM (cases B and B1 used the same method, with different grid resolutions). The analysis grid had a 0.25 m spacing for case B, and 1.00 m for all the other cases.

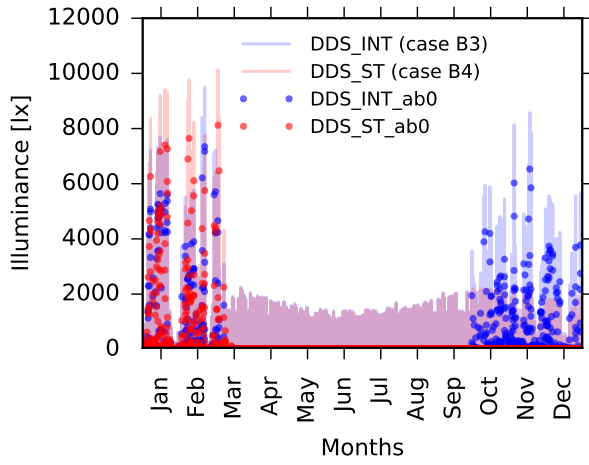


Figure 8: Illuminance values averaged over the working plane for each hour of the year. Two of the DAYSIM modes are compared, DDS with interpolation (blue) and DDS with Shadow Test (red). The values obtained for the global illumination are signed with lines in transparency, while the values obtained from direct sunlight are marked with circles.

This was analysed in greater detail by looking at the data in the illuminance profile generated from the simulation. The results are missing a big chunk of instances coming from the direct sunlight in the second part of the year, as shown in Fig. 8.

The sun position for the two halves of the year should be exactly symmetrical, with variations in illuminance results due only to the different sun intensities found in the weather file. The two cases shown in the figure both rely on the same representation of sun and sky, as per DDS scheme; hence, the issue cannot be caused by the assigned solar position. The fact that case B4 did not report any positive value from April onwards is believed to be related to the Shadow Test. The presence of venetian blinds might affect the performance of this method, although further analyses would be needed to confirm that this is the case, for example using shorter time steps rather than hourly.

Discussion

The ideal daylight simulation technique should be able to report truthfully all light that is transmitted and/or reflected through Complex Fenestration Systems, maintaining the visual pattern and effect that the system creates in the interior space. This level of accuracy is obviously in contrast with the short computation times required in any architectural and engineering practice, hence several approximations were introduced in all techniques for CBDM evaluations analysed in this study.

Some of the considered simulation methods were purposely created to model CFS, while other methods were not thought and validated for such systems. This study however, where non-specular venetian blinds were used, resulted in a generally good agreement between the methods, when comparing their outcome in terms of annual daylight metrics based on global illumination. For other light re-directing systems with highly reflective or highly specular materials, e.g. light-pipes, a number of ambient bounces beyond the capability of most methods would be required to accurately reproduce the system's light transfer properties. In those cases, the 3- and 5-phase methods with an appropriate BSDF would likely be the only possible solution.

Annual daylight metrics that are based on direct sunlight only, e.g. ASE, are characterised by significant uncertainty, caused by several factors. First of all, the representation of the sun is profoundly different in the considered methods, with solid angles ranging from about 14 degrees (e.g. in the 2-phase method) to 0.5 degrees (e.g. in the 5-phase method). Another influencing parameter is the resolution of the analysis grid, which appears to have a non-linear relationship with ASE values; the same simulation method (DAYSIM v4) led to different results when using a 0.25 m spaced grid (ASE = 15.4%) and a 1.00 m spaced one (ASE = 1.4%). This type of metrics is not robust enough, at the moment, to be considered for daylight performance evaluations, whether this is aimed at overheating or glare assessments.

Furthermore, there is a conceptual difference in the

definition of *direct light* among simulation methods, related to the use of either deterministic or stochastic sampling methods to account for the sun contribution and to the use of BSDF. Traditionally, running *rtrace* or *rpict* using `-ab 0` meant that only materials with the `light` modifier could be sampled, and any ambient stochastic calculation was automatically switched off. With the introduction of *rcontrib*, everything is traced stochastically and whenever a `glow` source needs to be ‘found’ (as in the 2-phase method and for the 3-phase method view matrix) or any off-angle ray needs to be accounted for within a BSDF (in a 5-phase method simulation), `-ab` needs to be set at 1. The direct sunlight is not necessarily traced on a straight line from the view point (or sensor point) to the light source any more, but could be slightly re-directed by the fenestration system and still be counted as direct light.

Instructions about CBDM simulation and metric calculation as given by the Illuminating Engineering Society (2012) become difficult to interpret. While earlier in the text this document suggests the use of the 3-phase method, when explaining the ASE calculation procedure, the following paragraph is presented:

In the Radiance software, direct sunlight is calculated using a “zero-bounce” simulation, with only the direct beam from the sun accounted for, where any sensor seeing 1000 lux or more (for $ASE_{1000,250H}$) is counted as being in “direct sunlight”.

Which one is the ‘correct’ definition of direct sunlight cannot be established here, as none of the analysed methods can be considered a reliable benchmark for CBDM evaluations of spaces with CFS applied. While in previous studies the 4-component method was used as benchmark, as the investigated spaces were modelled with clear glazing only (Brembilla et al., 2015; Brembilla, 2016), its validity cannot be assumed when venetian blinds are present. Further research is however planned in order to establish if a correlation exists between any of the existing simulation methods and assessments carried out in real spaces.

Conclusion

This paper investigated and compared the outcomes of five different techniques to perform Climate-Based Daylight Modelling (CBDM) evaluations when Complex Fenestration System (CFS) are present. Additionally, for three of these techniques, multiple variations in their application were explored and compared. Results show that, when using annual metrics that are calculated considering global illumination, there is a general agreement between all the considered methods. On the opposite hand, when annual daylight metrics are based on the direct sunlight contribution only, the results are highly dependent on the

chosen method. Annual Sunlight Exposure (ASE) in particular was found to lack robustness, due to several factors. The strict definition of ‘direct sunlight’ can also be considered flawed, in view of the most recent simulation techniques that include ‘re-directed sunlight’ too.

Acknowledgement

Ms. Brembilla acknowledges the support of EPSRC and industrial partner Arup, and Ms. Chi Pool the support of IUACC, CONACYT and Erasmus+. Dr. Hopfe and Prof. Mardaljevic acknowledge the support of Loughborough University.

Data Access

The data collected and generated for this work can be accessed via the Loughborough University repository (DOI: 10.17028/rd.lboro.4650205).

References

- Bourgeois, D., C. F. Reinhart, and G. Ward (2008, jan). Standard daylight coefficient model for dynamic daylighting simulations. *Building Research & Information* 36(1), 68–82.
- Brembilla, E. (2016). Applicability of Climate-Based Daylight Modelling. *Young Lighter of the Year*.
- Brembilla, E., J. Mardaljevic, and C. J. Hopfe (2015). Sensitivity Analysis studying the impact of reflectance values assigned in Climate-Based Daylight Modelling. In *Proceedings of BS2015: 14th Conference of IBPSA*, Hyderabad.
- Drosou, N., E. Brembilla, J. Mardaljevic, and V. Haines (2016, jul). Reality Bites: Measuring Actual Daylighting Performance in Classrooms. In *PLEA 2016: 32nd International Conference on Passive and Low Energy Architecture*, Los Angeles, CA, USA.
- Education Funding Agency (2014). EFA Daylight Design Guide Rev02. Technical Report January, Education Funding Agency, London, UK.
- Illuminating Engineering Society (2012). Approved Method: IES Spatial Daylight Autonomy (sDA) and Annual Sunlight Exposure (ASE). *IES LM-83-12*.
- Lawrence Berkeley National Laboratory (2013). EnergyPlus engineering reference. Technical report.
- Mardaljevic, J. (2000). *Daylight Simulation: Validation, Sky Models and Daylight Coefficients*. Ph. D. thesis, De Montfort University, Leicester, UK.
- McNeil, A. (2013). The Five-Phase Method for Simulating Complex Fenestration with Radiance. Technical Report August.

- McNeil, a., C. Jonsson, D. Appelfeld, G. Ward, and E. Lee (2013). A validation of a ray-tracing tool used to generate bi-directional scattering distribution functions for complex fenestration systems. *Solar Energy* 98, 404–414.
- McNeil, A. and E. Lee (2013, jan). A validation of the Radiance three-phase simulation method for modelling annual daylight performance of optically complex fenestration systems. *Journal of Building Performance Simulation* 6(1), 24–37.
- Mitchell, R., C. Kohler, L. Zhu, D. Arasteh, J. Carmody, C. Huizenga, and D. Curcija (2011). THERM 6.3/WINDOW 6.3 NFRC Simulation Manual. Technical report, LBNL-48255, Lawrence Berkeley National Laboratory, Berkeley, CA.
- Molina, G., W. Bustamante, J. Rao, P. Fazio, and S. Vera (2015). Evaluation of radiance’s genBSDF capability to assess solar bidirectional properties of complex fenestration systems. *Journal of Building Performance Simulation* 8(4), 216–225.
- Reinhart, C. F. (2001). *Daylight availability and manual lighting control in office buildings: Simulation studies and analysis of measurement*. Ph. D. thesis, University of Karlsruhe, Germany.
- Reinhart, C. F. and M. Andersen (2006). Development and validation of a Radiance model for a translucent panel. *Energy and Buildings* 38(7), 890–904.
- Reinhart, C. F. and S. Herkel (2000). The simulation of annual daylight illuminance distributions – a state-of-the-art comparison of six RADIANCE-based methods. *Energy and Buildings* 32(2), 167–187.
- Reinhart, C. F. and O. Walkenhorst (2001). Validation of dynamic RADIANCE-based daylight simulations for a test office with external blinds. *Energy and Buildings* 33(7), 683–697.
- Saxena, M., G. Ward, T. Perry, L. Heschong, and R. Higa (2010). Dynamic Radiance - Predicting annual daylighting with variable fenestration optics using BSDFs. In *Proceedings of SimBuild*, pp. 402–409.
- Tregenza, P. R. (1987, jan). Subdivision of the sky hemisphere for luminance measurements. *Lighting Research and Technology* 19(1), 13–14.
- Tsangrassoulis, A. and V. Bourdakis (2003). Comparison of radiosity and ray-tracing techniques with a practical design procedure for the prediction of daylight levels in atria. *Renewable Energy* 28(13), 2157–2162.
- US Green Building Council (USGBC) (2013). LEED Reference Guide for Building Design and Construction, LEED V4. Technical report, USGBC, Washington DC, USA.
- Ward Larson, G., C. Ehrlich, J. Mardaljevic, and R. Shakespeare (1998). *Rendering with Radiance: A Practical Tool for Global Illumination*. ACM SIGGRAPH Orlando, U.